Formation and control of a correlated exciton two-qubit system in a coupled quantum dot

Keishiro Goshima,[1,2,*] Kazuhiro Komori,[1,2] Takeyoshi Sugaya,[1,2] and Toshihide Takagahara[3]
[1]*National Institute of Advanced Industrial Science and Technology (AIST), 1-1-1 Umezono, Tsukuba, Ibaraki 305-8568, Japan*
[2]*CREST, Japan Science and Technology Corporation (JST), 1-6-1 Takezono, Tsukuba 305-0032, Japan*
[3]*Department of Electronics and Information Science, Kyoto Institute of Technology, Hashigami, Matsugasaki, Sakyo, Kyoto 606-8585, Japan*
(Received 25 September 2008; published 14 May 2009)

We have proposed the basic device structures for an all-optical controlled two-qubit quantum logic gate using two excitons confined in InAs/GaAs coupled quantum dots (CQDs). A two-qubit quantum logic gate is constructed using a correlated two-exciton system. This simplest two-qubit system involves four states such as the crystal ground states, two distinguishable exciton states, and a correlated-exciton-molecule state consisting of two excitons. The formation of this correlated-exciton-molecule state, which consists of two different excitons in a CQD, is the most important and difficult technology. In this study, we demonstrate the formation of the four states involving this correlated-exciton-molecule state and confirm two-qubit exciton system in CQDs. Moreover, we show that a correlated exciton molecule is created by employing a cascade process.

DOI: 10.1103/PhysRevB.79.205313 PACS number(s): 78.67.Hc, 78.66.Fd, 71.35.−y

I. INTRODUCTION

The realization of solid-state quantum information processing devices[1,2] requires two fundamental quantum logic gates, namely, a rotation gate (one qubit) and a controlled rotation gate (two qubit).[3] An electrically controlled device utilizing charge or flux in a superconductor[4] and an optically controlled device utilizing excitons in a semiconductor nanostructure[5,6] are two promising candidates for solid-state quantum logic gates. Optically controlled devices such as exciton qubits have the advantage of ultrahigh-speed operation. As regards exciton quantum logic gates, optical control of the exciton Rabi oscillation in a single quantum dot (SQD) has been considered as an elementary technique for realizing one-qubit operation.[5] For one-qubit gates, exciton Rabi oscillation in InGaAs/GaAs quantum dots (QDs) (Refs. 7–9) and InGaAs/AlGaAs QDs (Ref. 10) has been reported. In addition, our group has successfully demonstrated the Rabi oscillation of excitons in SQD (Ref. 11) and CQD (Ref. 12) systems. With respect to two-qubit exciton quantum logic gates, the entanglement of excitons in SQD has been demonstrated[13] and optically driven QDs have been proposed as quantum information system.[5] Chen *et al.*[14] have proposed the four-level system using exciton and biexciton in SQD, and Li *et al.*[15] have already demonstrated the Rabi oscillation of a exciton and a biexciton in a single GaAs/AlGaAs QD using the exciton-biexciton correlation. However, a single QD is difficult to a scalable device structure and is unsuitable for multiqubit devices. Therefore, the development of scalable device structures is very important as the next step toward realizing exciton-based multiqubit quantum logic gates. Multiqubit quantum logic gates using CQD have been proposed and the NMR class scalability was theoretically demonstrated, however, formation and control of correlated exciton two-qubit system have not been demonstrated yet.[5] We have fabricated and investigated the two-qubit logic gates using the correlated excitons in a CQD.[16–18] This simplest two-qubit system involves four states such as the crystal ground states ($|00\rangle$), two distinguishable exciton states ($|01\rangle$ or $|10\rangle$), and a correlated-exciton-molecule state ($|11\rangle$) consisting of two excitons as shown in Fig. 1(a). In this four-level two-qubit exciton system ($|00\rangle$, $|10\rangle$, $|01\rangle$, $|11\rangle$), the most important and difficult technology for the realization of two-qubit quantum logic gates is the formation of new states of the correlated-exciton-molecule state $|11\rangle$ using the exciton confined in each quantum dot of a CQD, and the formation of exciton correlation ($\Delta E \neq 0$). We have already demonstrated the creation of exciton-molecule states in CQDs.[16] However, it was not clear whether or not these states were two-qubit exciton system and four-level exciton system.

In this paper, we showed the two-qubit system involving four states using two experimental methods. Furthermore, we demonstrated the optical control of the two-qubit state of a correlated exciton molecule using an optical cascade process. We confirmed the validity of the following three statements. (1) Correlated-exciton-molecule states are created by two individual excitons and the binding energy of a correlated-exciton molecule is the same for both paths in two types of cascade process. (2) The spin-selection rule for two excitons is satisfied in the formation process of a correlated-exciton molecule. (3) A correlated-exciton-molecule state is created by the cascade process from the crystal ground state via the one-exciton state to the correlated exciton state.

Figures 1(a) and 1(b) show the transition-energy diagram of an entangled two-qubit exciton system using a CQD and a structural model with an scanning transmission electron microscope (STEM) image, respectively. Also, a model of the two-qubit exciton states of CQDs, where $|00\rangle$, $|01\rangle$ and $|10\rangle$, $|11\rangle$ are the crystal ground state, one-exciton state, and two-exciton states of the CQDs, respectively, are shown in Fig. 1(c). In the following, we name the $|11\rangle$ state as the correlated-exciton-molecule state, where the two different excitons confined in each quantum dot form new energy states by exciton-exciton interaction. Also we name the $|02\rangle$ or $|20\rangle$ state as the biexciton state where two excitons are confined in one quantum dot.

The transition energy between the crystal ground state ($|00\rangle$) and the one-exciton state ($|01\rangle$) is E_2, and that between the one-exciton state ($|10\rangle$) and the correlated-exciton-molecule state ($|11\rangle$) is $E_2-\Delta E$, where ΔE is the binding-energy shift caused by the formation of the correlated exci-

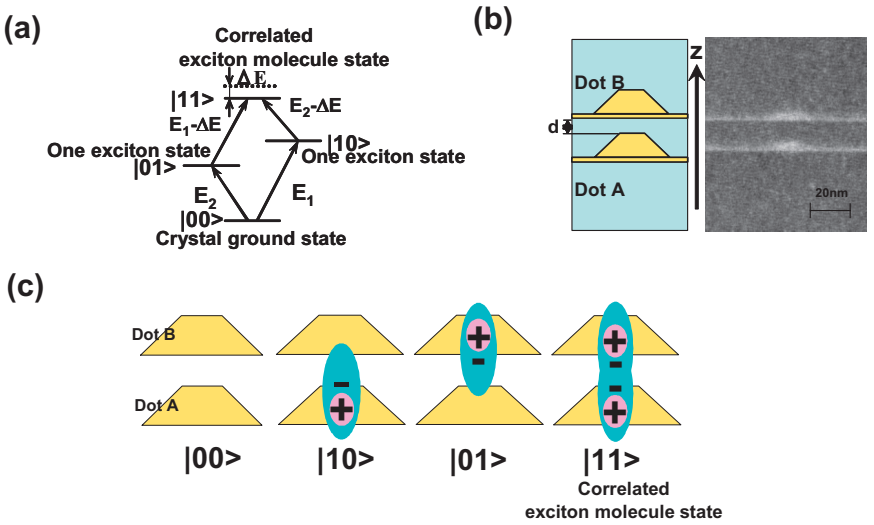

FIG. 1. (Color) Diagram of exciton two-qubit system using: (a) a CQD, (b) STEM image of InAs/GaAs CQDs, and (c) exciton four-level diagram with a CQD system, where α,β (=0 or 1) of $|\alpha,\beta\rangle$ shows the exciton states of QD-*A* and QD-*B*, respectively. $|00\rangle$, $|01\rangle$, $|10\rangle$, and $|11\rangle$ denote the crystal ground state, the *Xa*-exciton state, the *Xb*-exciton state, and the correlated-exciton-molecule state consisting of *Xa* and *Xb* excitons, respectively. ΔE indicates the binding energy of the correlated exciton molecule.

ton molecule. The transition energies of other excitation processes, namely, $|00\rangle \rightarrow |10\rangle$ and $|01\rangle \rightarrow |11\rangle$, correspond to E_1 and $E_1-\Delta E$, respectively. In two-qubit exciton system, the energy shift (ΔE) of $E_1-\Delta E$ should be the same as that of $E_2-\Delta E$ as shown in Fig. 1(a). The operation process of two-qubit logic gate using these four states is shown as follows. First, the ground state of $|00\rangle$ is optically excited to the state $|00\rangle+|01\rangle$ by applying a $\pi/2$ pulse with center frequency E_1. Second, the state $|00\rangle+|01\rangle$ is excited to the state $|00\rangle+|11\rangle$ by applying a π pulse with center frequency $E_2-\Delta E$. Note that the state $|00\rangle$ dose not evolve under the π pulse because of a detuning of ΔE. Now if $\Delta E=0$, the state $|00\rangle$ would also evolve to $|01\rangle$ under the π pulse, giving the two-qubit final state $|01\rangle+|11\rangle$ which is separable.

If there is no energy shift ΔE caused by the exciton-exciton interaction, the four-level two-qubit system can be factorized as two isolated one-qubit systems without any entanglement between the excitons. If a one-exciton state $|01\rangle$ or $|10\rangle$ is prepared and another exciton state is excited within a time Δt of exciton lifetime, then the entangled exciton states of $|11\rangle$ are realized in the CQD systems. The entangled four-level two-qubit exciton system cannot be factorized and two excitons are entangled owing to the existence of an energy shift of $\Delta E \neq 0$.[13]

II. SAMPLE AND EXPERIMENTAL SETUP

The methods employed to fabricate the samples used in the experiments were the same as those reported in our previous work.[18] The self-organized InAs QD samples were embedded in an *i*-GaAs matrix grown by molecular beam epitaxy with the indium-flush method.[19,20] Using the stacking growth technique, we obtained a CQD sample where two QDs were coupled in the growth direction with a barrier of thickness *d* between them, as shown in the cross-sectional STEM image in Fig. 1(b). We chose a *d* value of 5 nm to satisfy the requirements that (1) a hole is localized in each quantum dot to confine the excitons and (2) an electron is delocalized and weakly coupled between the quantum dots to realize biexcitonic coupling between the two different excitons confined in each quantum dot.[16]

For the spectroscopy of the single CQDs, titanium masks with apertures of 0.2–0.5 $\mu m\phi$ were formed on the sample surface by electron-beam lithography, where the in-plane QD density was as low as 30 pc s/μm^2 in order to obtain one CQD in the aperture. The CQD samples were cooled to 6 K in a liquid helium cryostat and excited by a continuous wave tunable Ti:sapphire laser. Luminescence from the QDs was collected through a microscope objective lens with a large numerical aperture (spot diameter ~2 $\mu m\phi$) led into a 1-m-double monochromator and detected with a cooled charge coupled device array detector whose spectral resolution was ~20 μeV.

III. RESULTS AND DISCUSSION

Figure 2(a) shows a micro photoluminescence (PL) spectrum from a CQD with $d=5$ nm used in this work. The PL spectrum has two groups of *Xa* and *Xb* with an energy separation of about 15–20 meV owing to quantum mechanical coupling,[16] where the suffixes "*a*" and "*b*" indicate the antibonding and bonding states, respectively. Also, each PL group consists of two peaks separated by 2–5 meV in which the lower- and higher-energy peaks are indicated as *Xa*(*Xb*) and *X*2*a*(*X*2*b*), respectively. Measurement of the spin selective optical excitation reveals that the *X*2*a* and *X*2*b* peaks originate from excitons with a *p*-like hole excited state.[17,18] In contrast, the *Xa* and *Xb* peaks originate from excitons with an *s*-like hole ground state. This is because the wave functions of the hole are not coupled with the neighboring QD due to the large effective mass of the hole, which leads to the small energy level separation.[17,18]

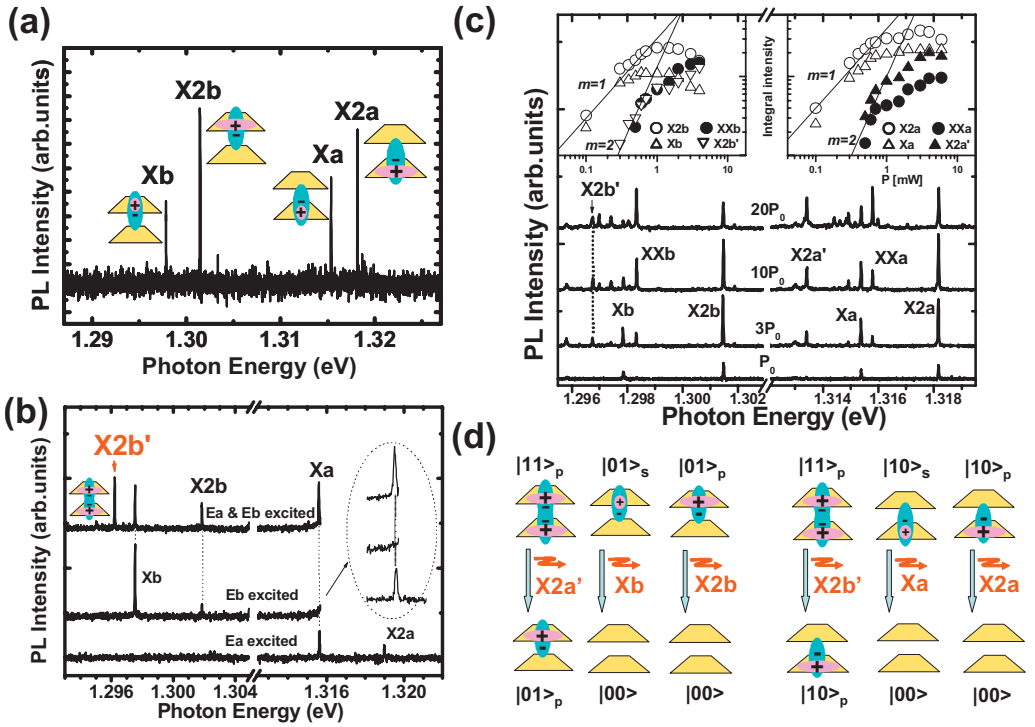

FIG. 2. (Color) PL spectra of a CQD. The *Xa* and *Xb* peaks originate from the antibonding and bondinglike states in a CQD, respectively. The *X2a* and *X2b* peaks originate from the antibonding and bondinglike states with the excited state of a hole in a CQD. (a) The PL spectrum of CQDs excited at 1.41 eV (absorption band of wetting layer) for which the excitation intensity was set sufficiently low such that multiple excitons could not be excited. (b) PL spectra of a CQD using one-color and two-color excitations. The inherent excitation at the *Ea* (*Eb*) energy yielded only a $|10\rangle$ state ($|01\rangle$ state) emission. (c) The one-color excitation-power dependence of the PL spectra, where the excitation energy and power P_0 are 1.41 eV and 300 μW, respectively. The inset shows integral PL intensity as a function of excitation power, where m indicates the exponent to the excitation power. $m=1$ ($m=2$) indicates the linear (quadratic) power dependence. Four peaks (*Xa*, *X2a*, *Xb*, and *X2b*) are proportional to linear-power dependence ($m=1$). The other four peaks (*XXa*, *X2a′*, *XXb*, and *X2b′*) are proportional to the quadratic-power dependence ($m=2$). (d) The relationship of the PL peaks to the exciton states in a CQD. PL peaks of *X2b′*, *Xb*, *X2b*, *X2a′*, *Xa*, and *X2a* correspond to $|11\rangle p \rightarrow |01\rangle p$, $|01\rangle s \rightarrow |00\rangle$, $|01\rangle p \rightarrow |00\rangle$, $|11\rangle p \rightarrow |10\rangle p$, $|10\rangle s \rightarrow |00\rangle$, and $|10\rangle p \rightarrow |00\rangle$, respectively.

In the following, the one-exciton state created by an electron of the bondinglike state and a hole of the *s*-like (*p*-like) state represents the $|01\rangle s$ ($|01\rangle p$) state, and that created by an electron of the antibondinglike state and a hole of the *s*-like (*p*-like) state represents the $|10\rangle s$($|10\rangle p$) state. Also, the $|10\rangle$ and $|01\rangle$ states represent all $|10\rangle$ states including the $|10\rangle p$ and $|10\rangle s$ states, and all $|01\rangle$ states including the $|01\rangle p$ and $|01\rangle s$ states, respectively.

Figure 2(a) shows the relation between the PL emission and the energy transition of a two-qubit system. The PL peaks of *Xa*, *Xb*, *X2a*, and *X2b* originate from the one-exciton states of $|10\rangle s$, $|01\rangle s$, $|10\rangle p$, and $|01\rangle p$, respectively.

In our photoluminescence excitation (PLE) measurements of a CQD system, we found inherent excited states of *Ea*(=1.3231 eV) and *Eb*(=1.3392 eV) for the $|01\rangle$ and $|10\rangle$ states, respectively.[15,18] Thus, the creation of excitons of the $|01\rangle$ and $|10\rangle$ states can be controlled individually using two laser sources. For example, when we pump at the inherent excited state of *Ea* (*Eb*), the $|10\rangle$ ($|01\rangle$) state can be created but the $|01\rangle$ ($|10\rangle$) state cannot be created. Figure 2(b) shows the PL spectra under individual (one-color) excitation or simultaneous (two-color) excitation conditions using energy selective excitation as mentioned above. The excitation at the *Ea* (*Eb*) energy yielded only a $|10\rangle$ ($|01\rangle$) emission as shown in the center (bottom) of Fig. 2(b).

When the $|10\rangle$ and $|01\rangle$ states were excited simultaneously by using two-color excitation (both *Ea* and *Eb*), a new peak appeared on the lower energy side of the *Xb* peak in the spectrum (labeled *X2b′* at the top of the figure). This observation directly reveals the existence of an exciton molecule in a CQD system.

To clarify the origin of the *X2b′* peak, we investigated the excitation-power dependence on PL intensity of all the multiple exciton peaks. First, we measured the one-color excitation-power dependence of the PL intensities, where the excitation laser energy is fixed at the wetting-layer energy, as shown in Fig. 2(c). We observed four PL peaks under weak-power excitation conditions as shown in the bottom graph of Fig. 2(c). These four peaks (*Xa*, *X2a*, *Xb*, and *X2b*) originated from one-exciton states owing to the linear-power dependence on excitation power. With a strong excitation density, four new peaks (*XXa*, *X2a′*, *XXb*, and *X2b′*) appeared on the lower energy side of the *Xa*, *X2a*, *Xb*, and *X2b* excitons. These four peaks exhibit a quadratic dependence on excitation power, which implies that two excitons contribute to form these new peaks. The possible transitions of these peaks, which are investigated in the experiments described below, are shown in Fig. 2(d).

We performed three experiments to obtain evidence that the correlated exciton molecule consists of two different ex-

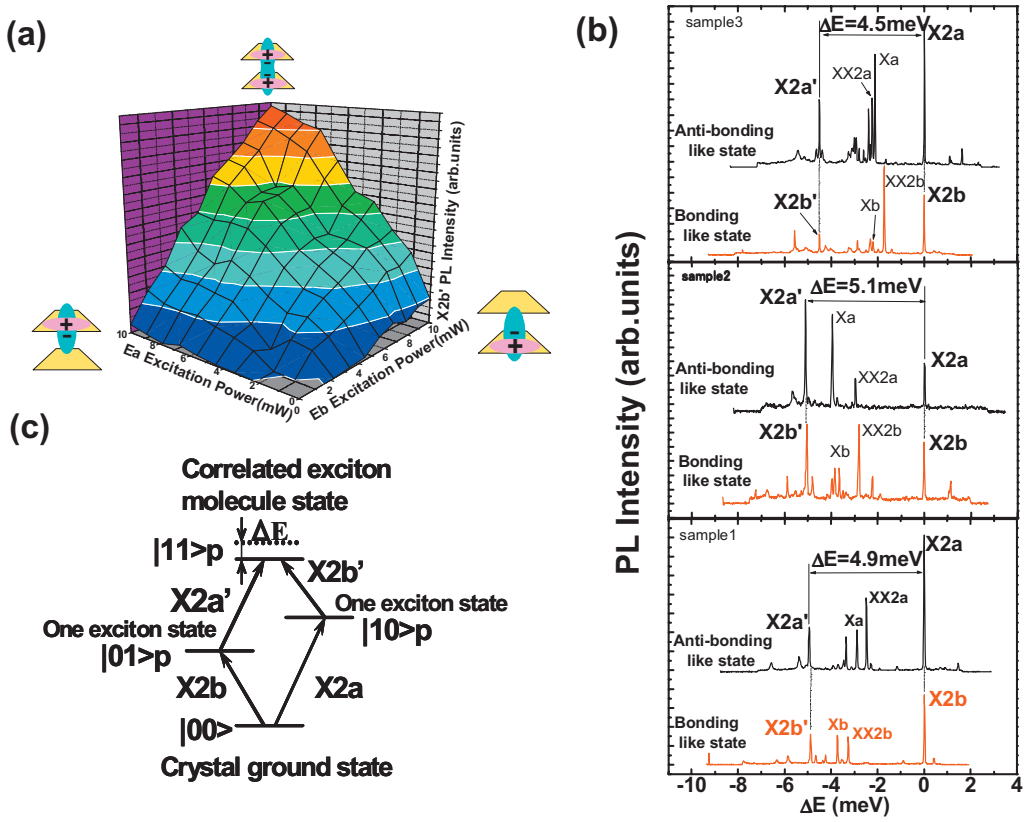

FIG. 3. (Color) PL intensity and PL spectrum of correlated exciton molecule (a) PL spectrum of one- and two-exciton states excited at 1.41 eV with strong optical excitation for the three different CQD samples. The energy shifts (ΔE) between $X2aX2a'$ and $X2bX2b'$ almost all have the same value (ΔE=4.6, 5.1, and 4.9 meV), respectively. Inset: the $X2a'$ and ($X2b'$) peaks correspond to the energy of the $|11\rangle p \rightarrow |10\rangle p$ ($|11\rangle p \rightarrow |01\rangle p$) state. (b) Exciton four-level diagram in a CQD based on these results. The one-exciton state ($|00\rangle \rightarrow |01\rangle p$ or $|00\rangle \rightarrow |10\rangle p$) corresponds to the $X2a$ and $X2b$ PL peaks, respectively. The correlated-exciton-molecule state ($|11\rangle p \rightarrow |10\rangle p$ or $|11\rangle p \rightarrow |01\rangle p$) corresponds to the $X2a'$ and $X2b'$ peaks.

citons. The first was to determine the two-color excitation-power dependence of the $X2b'$ PL intensity. In the second, we measured the energy difference between the PL peaks of single exciton states of $Xa(Xb)$ and that of correlated-exciton-molecule states $Xa'(Xb')$. The third experiment involved the spin and energy selective excitation of the PL intensity of the correlated exciton molecule.

First, we measured the two-color excitation-power dependence on the intensity of the $X2b'$ PL peak, as shown in Fig. 3(a), where the two-color excitation energies were fixed at Ea and Eb as inherent excited states. If the $X2b'$ peak originates from the biexciton state $|02\rangle$ of Xb itself, the PL intensity of $X2b'$ should strongly depend only on the Eb excitation, while if $X2b'$ originates from the correlated-exciton-molecule state $|11\rangle$, the PL intensity of $X2b'$ should depend on both Ea and Eb excitation. The result showed that the $X2b'$ PL intensity depends on both Ea and Eb excitation, which reveals that the $X2b'$ peak originates from the correlated-exciton-molecule state of $|11\rangle$ created by two individual excitons.

Second, we measured the PL spectra under strong optical excitation at the wetting layer energy as shown in Fig. 3(b), where the horizontal axis (ΔE) indicates the energy measured from the $X2a$ and $X2b$ peaks, namely, E-$X2a$ and E-$X2b$, respectively. A noteworthy characteristic of the two-qubit exciton system is that the energy difference between $X2a$ and $X2a'$, which corresponds to a correlated-exciton-molecule binding energy, must be the same as that between $X2b$ and $X2b'$. In passing, we observed the same feature in several other CQD samples as shown in Fig. 3(b). From these results, we confirmed that a two-qubit exciton system is realized in our CQDs. Figure 3(c) shows the energy diagram of the two-qubit exciton system in our CQDs. The four-level system is created from two different excitons, $|10\rangle p$ and $|01\rangle p$, and the energy of the biexcitonic interaction ΔE of the correlated exciton molecule corresponds to 4.9–5.1 (meV) for five measured samples. Therefore, the $X2a'(X2b')$ peak corresponds to the energy difference between the $|11\rangle p$ state and the $|10\rangle p$ state ($|11\rangle p$ state and $|01\rangle p$ state), respectively. These results provide evidence that the $X2b'$ and $X2a'$ peaks originate from the correlated-exciton-molecule state $|11\rangle p$ in a CQD.

Finally, we examined the exciton spin-selection rule in an exciton formation experiment, where the artificial exciton molecule $|11\rangle p$ could only be created by the two excitons in a CQD with antiparallel spin. In other words, if the $X2b'$ ($X2a'$) peak originates from the correlated exciton molecule, the PL intensity of $X2b'$ ($X2a'$) should depend on both polarized excitations (Ea and Eb) because a correlated exciton molecule can be created when two excitons ($|01\rangle p$ and $|10\rangle p$)

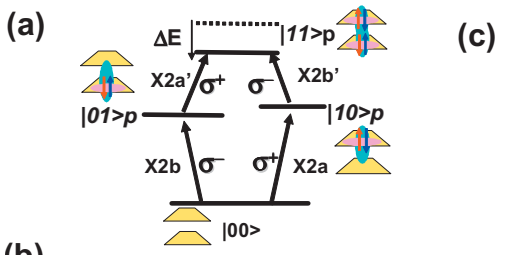

Polarized & selective excitation		Biexciton or correlated exciton molecule	
Xa, X2a (Ea)	Xb, X2b (Eb)	Biexciton	Correlated exciton molecule
Linear	Linear	"a"	"a"
σ+	σ+	"d"	"d"
σ−	σ+	"d"	"a"
σ+	σ−	"d"	"a"

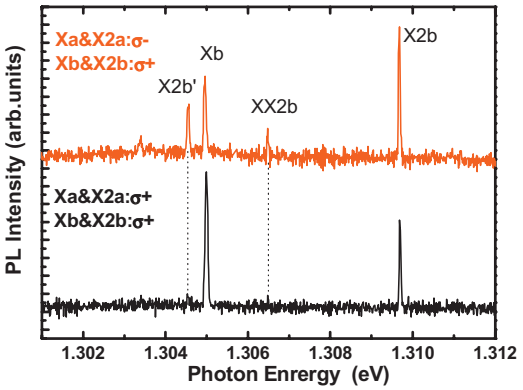

FIG. 4. (Color) PL spectrum with spin-selective excitation. (a) Exciton four-level system including the spin-selection rule and a table of the classification as a correlated exciton molecule or a biexciton using spin-polarized and selective excitation. (b) Appearance and disappearance table of a biexciton and a correlated exciton molecule which is expected from spin-selection rule. "*a*" and "*d*" shows appearance and disappearance of the PL peak, respectively. (c) PL spectrum of one- and two-exciton states in CQDs under both energy ($|10\rangle$ and $|01\rangle$) and spin-polarized selective excitation ($\sigma+$ and $\sigma-$). The upper PL shows antiparallel spin ($|10\rangle:\sigma-$ and $|01\rangle:\sigma+$) excitation. The lower PL shows parallel spin ($|10\rangle:\sigma+$ and $|01\rangle:\sigma+$) excitation. The $X2b'$ and XXb peaks appear only with antiparallel spin excitation.

have antiparallel spin. Therefore we investigated the XXb and $X2b'$ peaks using circular polarized and selective optical excitation. These approaches classify multiexcitons as correlated exciton molecules $|11\rangle$ and biexcitons $|20\rangle$ or $|02\rangle$. Figure 4(a) is a diagram of a four-level two-qubit exciton system of $|00\rangle$, $|01\rangle p$, $|10\rangle p$, and $|11\rangle p$ in CQDs including exciton spin, and Fig. 4(b) shows the condition table for the PL of a correlated exciton molecule and a biexciton, where "*a*" and "*d*" indicate the appear and disappear of the PL peak, respectively, for two color (Ea and Eb) and spin- ($\sigma+$ and $\sigma-$ and linear) selective excitation. Figure 4(c) shows the PL spectrum of XXb and $X2b'$ using two-color polarized and selective excitations under the weak excitation power of Ea and Eb, where the excitation power of the polarized Ea and Eb are same as that of linear Ea and Eb. We observed that the PL peaks of $X2b'$ and XXb only appeared with the polarized selective excitation of excited states of $X2a$ ($\sigma-$) and those of $X2b$ ($\sigma+$), respectively. Thus, we confirmed that the correlated exciton molecule can only be created from two excitons with antiparallel spins. Therefore, the PL peak of $X2b'$ was the ground state of the correlated exciton molecule originating from two different excitons $|01\rangle p$ and $|10\rangle p$ in a CQD and XXb was the excited state of the correlated exciton molecule. From the results of the PL spectra under strong excitation and the PL spectrum with spin-selective excitation, we obtained evidence that a correlated two-qubit exciton system consisting of a ground state $|00\rangle$, one-exciton states $|01\rangle p$ and $|10\rangle p$, and a correlated-exciton-molecule state $|11\rangle p$ can be created in CQDs.

As a next step, we attempted to realize the optical control of the two-qubit state of a correlated exciton molecule using an optical cascade process and investigated the transient carrier dynamics of a correlated exciton molecule. We performed the cascade optical process on the correlated exciton molecule by employing a two-color selective excitation measurement. In a correlated two-qubit exciton system with a crystal ground state $|00\rangle$, one-exciton states $|01\rangle p$ and $|10\rangle p$, and a correlated-exciton-molecule state $|11\rangle p$ as shown in Fig. 4(a), the correlated-exciton-molecule state should be created by the cascade process of $|00\rangle \rightarrow |10\rangle p \rightarrow |11\rangle p$ and this can be monitored by measuring the PL of $X2b'$ ($|11\rangle p \rightarrow |10\rangle p$).

The procedure for measuring the optical control of the two-qubit state is as follows. First, a continuous-wave (cw) pump light source is fixed at the first excited state of a one-exciton state [=1.339 eV($|01\rangle pe$)], which is excited constantly, as indicated by "pump1" in the Fig. 5(a) inset. The created $|01\rangle pe$ excitons relax to the ground state of the one-exciton state $|01\rangle p$ which indirectly creates the one-exciton state ($|00\rangle \rightarrow |01\rangle p$). Note that the excitation of $X2be$ energy could not create the $|10\rangle$ state series and the PL of $X2a$ and Xa did not appear. Then, the energy of the second pump is tuned to $X2a'$ [=1.3136 eV($X2a-\Delta E$)] energy using pulsed laser light, as indicated by "pump2," which is the directly tuned transition energy between the $|01\rangle p$ and $|11\rangle p$ states. Finally, we monitored the populations of the correlated-exciton-molecule state through the PL spectrum of $X2b'$, namely, the transition from the $|11\rangle p$ state to the $|10\rangle p$ state, as indicated by "PL3" in the inset of Fig. 5(a).

The result of the cascade optical excitation of a correlated-exciton-molecule is shown in Fig. 5(a), where the bottom graph shows one-color excitation ($|01\rangle pe$) and the middle and top graphs show two-color excitations with different excitation powers $P(X2a')$ of 5 and 15 mW, respectively.

We directly observed that the correlated-exciton-molecule state ($X2b'$) appeared only for certain two-color excitations

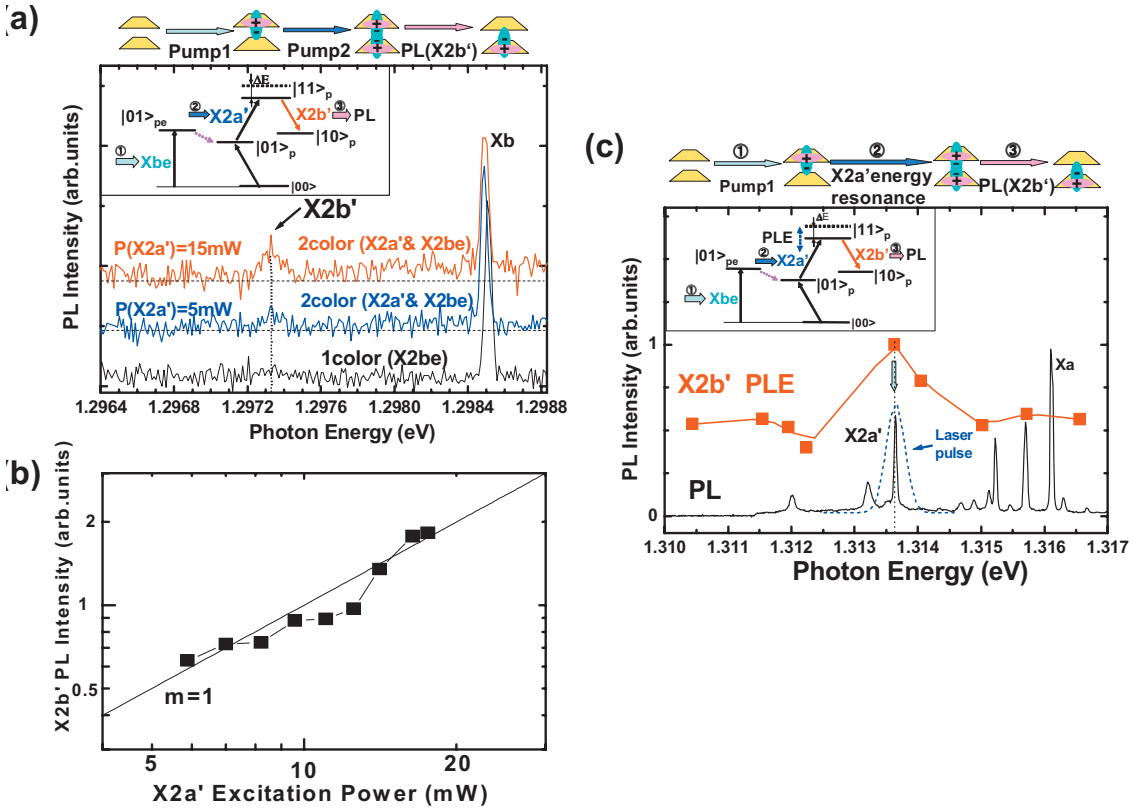

FIG. 5. (Color) PL and PLE spectra of cascade process with correlated exciton molecule: (a) Cascade process of correlated exciton molecule ($|11\rangle p$) using two-color excitation. The inset shows a schematic drawing of the configuration of the cascade process of an exciton four-level system using two-color excitation. A one-exciton state ($|00\rangle \rightarrow |10\rangle p$) is created by the first excitation ("pump1") and a correlated-exciton-molecule state ($|10\rangle p \rightarrow |11\rangle p$) is created by the second excitation ("pump2"), finally the PL of $X2b'$ ("PL3") is monitored ($|11\rangle p \rightarrow |01\rangle p$). The $X2b'$ peak appears only with two-color ($X2be$ and $X2a'$) excitation. (b) The $X2b'$ peak intensity increases in proportion to the linear-power dependence of $P(X2a')$. (c) The PLE spectrum of the $X2b'$ peak obtained using two-color excitation PLE measurement. PLE spectrum of $X2b'$ and PL spectra of Xa and $X2a'$ are shown by red and black line, respectively. Pulse spectrum of second-excitation pulse is shown in blue line. The $X2b'$ PLE peak energy agrees well with $X2a'$ PL energy. Inset: Schematic drawing of two-color PLE measurement of the four-level diagram in a CQD. The conditions for "pump1" and "PL3" are the same as in Fig. 5(a). The second excitation energy is varied from 1.31 to 1.317 eV.

of $X2be$ and $X2a'$ as shown in the top graph in Fig. 5(a). The PL intensity as a function of the $X2a'$ excitation power for $X2b'$ peaks is shown in Fig. 5(b). The PL intensity of $X2b'$ increases in proportional to the linear-power dependence of $X2a'$. To confirm that the $X2b'$ peak only appeared as a result of the cascade optical excitation, we undertook a two-color PLE measurement as shown in the inset in Fig. 5(c). First, a one-exciton state of $|01\rangle p$ was created by cw excitation at an energy of $X2be$ (=1.339 eV). Then, $X2a'$ was excited by a second light source whose energy was detuned from 1.3105 to 1.3165 eV for the two-color PLE measurement. We measured the PLE spectra of the $X2b'$ peak, and finally compared them with the PL spectra of the $X2a'$ peak as shown at the bottom of Fig. 5(c).

The measurement results are also shown in Fig. 5(c). We observed that the energy of the $X2b'$ PLE peak was consistent with that of the correlated exciton molecule of the $X2a'$ PL peak (1.3136 eV). These results showed that the correlated-exciton-molecule ($|11\rangle p$) state was created by the cascade optical excitation ($|00\rangle \rightarrow |01\rangle p \rightarrow |11\rangle p$). And, we succeeded in controlling the population of the two-qubit state of $|11\rangle p$ in a CQD system.

As further work, it will be important to demonstrate Rabi oscillation between the $|01\rangle$ and $|11\rangle$ states. In a two-qubit controlled rotation (CROT) gate, the target bit (first bit) is rotated through a π-pulse area, if and only if the control bit (second bit) is 1. To be more specific, a π pulse tuned to the $|01\rangle \rightarrow |11\rangle$ transition is chosen as the operational pulse for the CROT gate. When the input is only $|01\rangle$ the operational pulse will rotate the input to $|11\rangle$. Similarly, if an input of $|11\rangle$ is chosen the operational pulse will stimulate it down to $|01\rangle$.

IV. SUMMARY

In conclusion, we have proposed extending the basic device structure to multibit devices for optically controlled quantum computers using CQDs. And we have successfully demonstrated the formation and control of two-qubit exciton states consisting of two-qubit exciton system in CQDs. This shows that our device structure can be utilized as a two-qubit quantum logic gate, and demonstrates a two-qubit solid-state device structure that can enable us to realize both ultrafast optical control and multibit.

*ke-goshima@aist.go.jp

[1] D. Deutsch, Phys. Rev. D **44**, 3197 (1991).
[2] M. A. Nelsen and I. L. Chuang, *Quantum Computation and Quantum Information* (Cambridge University Press, Cambridge, England, 2000).
[3] A. Barenco, C. H. Bennett, R. Cleve, D. P. DiVincenzo, N. Margolus, P. Shor, T. Sleator, J. A. Smolin, and H. Weinfurter, Phys. Rev. A **52**, 3457 (1995).
[4] T. Yamamoto, Yu. A. Pashkin, O. Astafiev, Y. Nakamura, and J. S. Tsai, Nature (London) **425**, 941 (2003).
[5] E. Biolatti, R. C. Iotti, P. Zanardi, and F. Rossi, Phys. Rev. Lett. **85**, 5647 (2000).
[6] N. H. Bonadeo, J. Erland, D. Gammon, D. Park, D. S. Katzer, and D. G. Steel, Science **282**, 1473 (1998).
[7] H. Kamada, H. Gotoh, J. Temmyo, T. Takagahara, and H. Ando, Phys. Rev. Lett. **87**, 246401 (2001).
[8] H. Htoon, T. Takagahara, D. Kulik, O. Baklenov, A. L. Holmes, Jr., and C. K. Shih, Phys. Rev. Lett. **88**, 087401 (2002).
[9] J. M. Villas-Boas, S. E. Ulloa, and A. O. Govorov, Phys. Rev. Lett. **94**, 057404 (2005).
[10] T. H. Stievater, X. Li, D. G. Steel, D. Gammon, D. S. Katzer, D. Park, C. Piermarocchi, and L. J. Sham, Phys. Rev. Lett. **87**, 133603 (2001).
[11] K. Goshima, S. Yamauchi, K. Komori, I. Morohashi, A. Shikanai, and T. Sugaya, Jpn. J. Appl. Phys., Part 1 **45**, 3625 (2006).
[12] K. Goshima, S. Yamauchi, K. Komori, I. Morohashi, A. Shikanai, and T. Sugaya, Jpn. J. Appl. Phys., Part 1 **46**, 2626 (2007).
[13] G. Chen, N. H. Bonadeo, D. G. Steel, D. Gammon, D. S. Katzer, D. Park, and L. J. Sham, Science **289**, 1906 (2000).
[14] G. Chen, T. H. Stievater, E. T. Batteh, X. Li, D. G. Steel, D. Gammon, D. S. Katzer, D. Park, and L. J. Sham, Phys. Rev. Lett. **88**, 117901 (2002).
[15] X. Li, Y. Wu, D. Steel, D. Gammon, T. H. Stievater, D. S. Katzer, D. Park, C. Piermarocchi, and L. J. Sham, Science **301**, 809 (2003).
[16] K. Goshima, S. Yamauchi, K. Komori, I. Morohashi, and T. Sugaya, Appl. Phys. Lett. **87**, 253110 (2005).
[17] S. Yamauchi, K. Komori, I. Morohashi, K. Goshima, and T. Sugaya, Appl. Phys. Lett. **87**, 182103 (2005).
[18] S. Yamauchi, K. Komori, I. Morohashi, K. Goshima, and T. Sugaya, J. Appl. Phys. **99**, 033522 (2006).
[19] Z. R. Wasilewski, S. Fafard, and J. P. McCaffrey, J. Cryst. Growth **201-202**, 1131 (1999); T. Takagahara, Phys. Rev. B **62**, 16840 (2000).
[20] Q. Xie, A. Madhukar, P. Chen, and N. P. Kobayashi, Phys. Rev. Lett. **75**, 2542 (1995).